



Image-based method for the investigation of low flexure rigidity materials

Jovita Dargienė*, Dalia Lukšaitė, and Jurgita Domskienė

Department of Clothing and Polymer Products Technologies, Faculty of Design and Technologies, Kaunas University of Technology, Studentų 56, LT-51424 Kaunas, Lithuania

Received 8 November 2011, revised 18 June 2012, accepted 20 June 2012, available online 30 August 2012

Abstract. The image analysis method is used for the evaluation of the mechanical behaviour of bias stretched woven material and determination of the zones and values of local deformations of the specimen. To demonstrate the capabilities and reliability of the proposed image analysis method, the simplest and most commonly used uniaxial tensile test was chosen. Using the acquired images, local deformations of the specimen in transverse and longitudinal directions were estimated and regularities of the variation of uniform deformation zones were assessed.

Comparison of the behaviour of materials shows that increase in bending rigidity changes the deformation character of materials. For non-laminated low flexure rigidity materials the formation of localized deformation zones was estimated at primary stages of deformation, as in the case of stiffer laminated fabric the zones of uniform deformations spread more and do not concentrate within the centre of the specimen. The different nature and shape of local deformation zones indicate that the behaviour of laminated materials is closer to that of isotropic materials.

The obtained results show that image analysis can describe the response of low flexure rigidity material to external forces. This method supplements the investigation process of woven materials, increases the accuracy of measurements, and determines the real-time local strains.

Key words: image analysis, local deformations, bias tension, woven material.

1. INTRODUCTION

Buckling is a phenomenon of the loss of the form stability of low flexure rigidity material when longitudinal tension and transverse compression stresses affect bias tensioned woven material. Due to the woven structure and anisotropic properties, parts of the specimen are unevenly tensioned and the strain is uniform throughout the specimen. The problem of material form instability is important for technical and architecture textiles when complex strains are applied to maintain three-dimensional form.

Current strain determination methods mostly assume that the strain is uniform throughout the specimen and it is difficult to evaluate the stress distribution of textiles. Non-contact methods such as holography, speckle [1,2], Moiré interferometry [3], and digital image analysis [4–15] are proposed for the evaluation of strain dis-

tribution. With different techniques and equipments it is possible to record real-time strain distribution fields. These methods are very useful for the study of the mechanical behaviour of materials and extend the results received by standard test methods, providing more information about the behaviour of the tested materials.

Some studies have used the non-contacting strain measuring technique to obtain the local strain values and zones of textiles. Image analysis has been applied under tensile testing of technical textile to assess the deformations at the tested strain rates [14], variation in the actual shear angle of the bias fabric [10], and homogeneity of shearing within the specimen [14], to describe three deformation phases and explain the large deformation mechanism and slippage phenomenon [6]. This method provides independent measurements and different studies confirm its effectiveness in textile investigation [13,15]. Image analysis is a suitably sensitive method for recording and measuring small deformations, however, the

* Corresponding author, jovita.dargiene@stud.ktu.lt

measurement of deformations is strongly related to the conditions of image acquisition and analysis algorithm. In some cases the surface properties and colour of the tested sample are a restriction to the use of the digital image analysis method. According to the investigations of many researchers, the methodology of image analysis has to be adapted for a particular problem.

The aim of this research is to use the image analysis method for evaluation of the mechanical behaviour of bias stretched woven material and to determine the zones and values of local deformations of the specimen for changing deformability when the movement of threads is restricted by fabric lamination.

2. MATERIALS

To demonstrate the capabilities and reliability of the chosen image analysis method, three different weave fabrics (Fig. 1) of the same composition (warp 70% cotton and 30% PES; weft 100% PES), the number of threads per unit length (warp 28 cm^{-1} , weft 20 cm^{-1}), and linear density (warp 39.9 tex, weft 18.1 tex) were chosen for research. Textiles were laminated with the “Poly-flex” membrane (a high-density polyethylene PEC) according to producer’s recommendations (temperature 165°C , time of pressing 20 s).

3. EXPERIMENTAL

For the uniaxial tensile test the universal testing machine Thinius Olsen was used at the upper clamp speed of 10 mm/min. Bias (45° to the warp thread system) rectangular specimens with the operating area of $50 \text{ mm} \times 100 \text{ mm}$ were prepared. For image analysis a regular grid of fill circles was printed on the specimen (Fig. 2a, b). In order to achieve good contrast, samples were printed in black colour on light fabric.

Two parts of different deformations A and B (Fig. 2c) were distinguished within the tensioned specimen. It is known that due to the restraints of woven sample thread systems within machine clamps, the

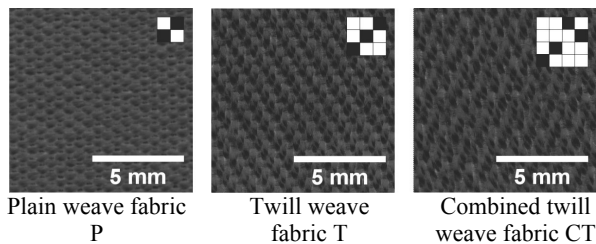


Fig. 1. The structure schemes of chosen materials.

deformation of zone A has been non-essential, and the highest deformations of the specimen have been determined within zone B. It is assumed that zone A remains constant during tension (the length of zone A $l_A = \text{const}$) and zone B elongates depending on the total specimen elongation ε , where the length of zone B $l_B + \varepsilon_i$ (Fig. 2c).

Images of the deformed specimen were recorded at certain times by the digital camera OLYMPUS E620 (resolution 4032×3024 pixels), which was located stationary in front of the specimen at a distance of $X = 350 \text{ mm}$ (Fig. 3). The centre of the camera lens was set in front of the tensioned specimen plane. Two light sources in the angle of 45° (300 W Philips halogen lamp, 3000 K) were placed at a distance of $X' = X'' = 350 \text{ mm}$. The images of the deformed specimen were acquired at every step of 5% of specimen elongation until 20%. For the digital image calibration, the ruler was placed at the same plane as the specimen.

Using the acquired images, local longitudinal and transverse deformations were estimated for the samples and regularities of variations in uniform deformation zones were assessed. The input images were converted to 8 bit greyscale images. To reduce the effect of noise, the Gaussian blur filter with a radius of $\sigma = 3$ was applied. Image processing by the threshold procedure was used to restore the grid of the deformed specimen in the image. The threshold value was determined as the mean value of the approximated histogram of a specimen image.

The specialized program *ImageJ* was supplemented by the developed subprogram *KTU_Image JD* and the height h and width b of each grid point were measured (Fig. 4). Measurements of the captured image during the calibration process were transferred to the desired metric units. The local deformations of the specimen were evaluated according to variation in the height h and width b of each grid point:

$$\Delta b_{ij} = \frac{b_0 - b_{ij}}{b_0} \times 100, \quad (1)$$

$$\Delta h_{ij} = \frac{h_0 - h_{ij}}{h_0} \times 100, \quad (2)$$

where b_0 – initial width of the grid point; h_0 – initial height of the grid point; b_{ij} , h_{ij} – value of grid point i deformation at the elongation moment j .

Investigations of the printed grid showed that the calculated variation in grid point height Δh_{ij} (Eq. 2) and width Δb_{ij} (Eq. 1) displays the actual place of local longitudinal and transverse displacements of the specimen.

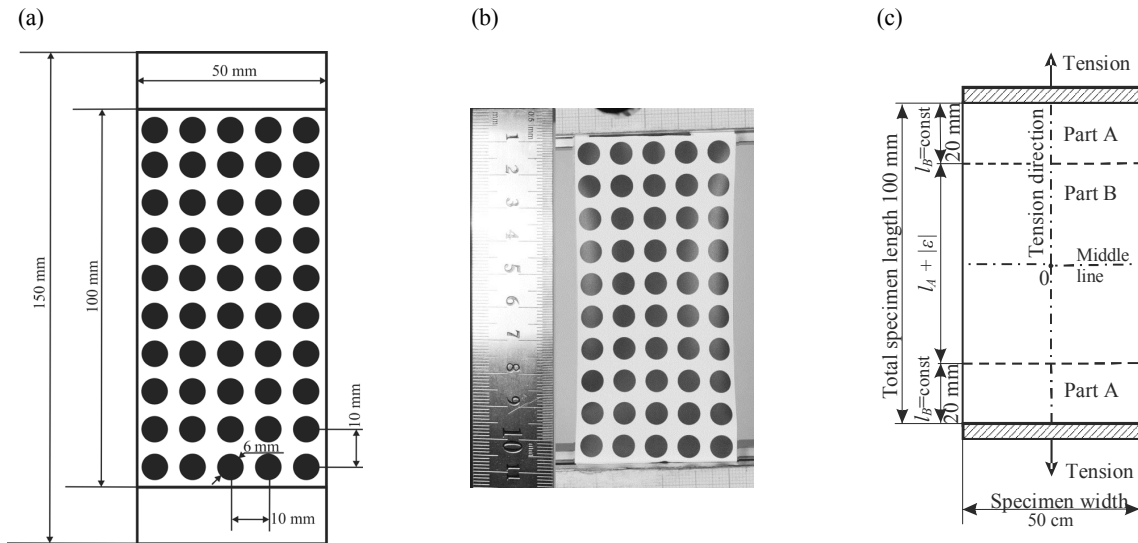


Fig. 2. The scheme of specimen preparation (a), acquired image of the printed specimen (b), separated parts of the bias tensioned specimen (c).

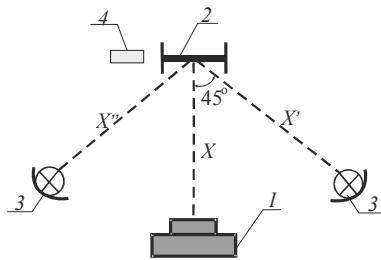


Fig. 3. The scheme of the experiment: 1 – digital camera, 2 – specimen, 3 – light source, 4 – ruler.

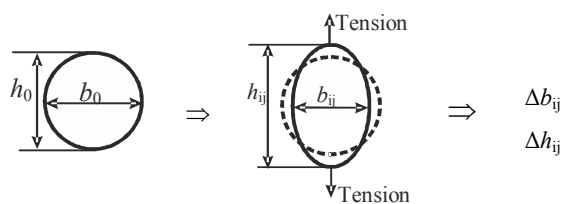


Fig. 4. The scheme of grid point height h and width b measurements.

4. RESULTS AND DISCUSSION

Surface density w of plain weave (P), twill weave (T), and combined twill weave (CT) materials increased several times after lamination, and relatively small increase occurred in their thickness S (Table 1). Lamination influenced mostly the bending rigidity B , which increased in plain weave (P) and twill weave (T) samples by 5 times and by 9 times in the lower flexure rigidity sample CT (Table 1).

Table 1. Properties of chosen fabrics and laminated fabrics

	Woven samples			Laminated woven samples		
	P	T	CT	PL	TL	CTL
Surface density w , g/m ²	155	153	155	370	346	349
Thickness S , mm	0.43	0.47	0.54	0.56	0.58	0.68
Bending rigidity B , μNm	11.3	11.1	7.6	167.10	101.12	87.89

Figure 5 shows tension curves $F - \epsilon$ of the selected fabrics (P, T, CT), lamination membrane L and laminated materials (PL, TL, CTL). In all cases laminated samples become stiffer and their tension curves are different from non-laminated fabric as partial limitation of thread flexibility is obtained during the lamination process. Lamination of the twill weave fabric T changed the deformation character within the tensile curve where performance specific for isotropic materials prevailed. The influence of lamination on the tensile behaviour of CT was not that intense. For the last case, during bonding of two materials CT and L of different tension character a new two-ply material CTL was composed and the behaviour of this material has shown an intermediate position between the curves of initial components (Fig. 5c).

Uneven deformations become evident during the primary deformation stage ($\epsilon_i = 5\%$) within specimens of stretched plain weave P, twill weave T, and combined twill weave CT (Table 2). Deformation zones of the P specimen are concentrated mostly within the centre of the specimen along the tensile axis, while the

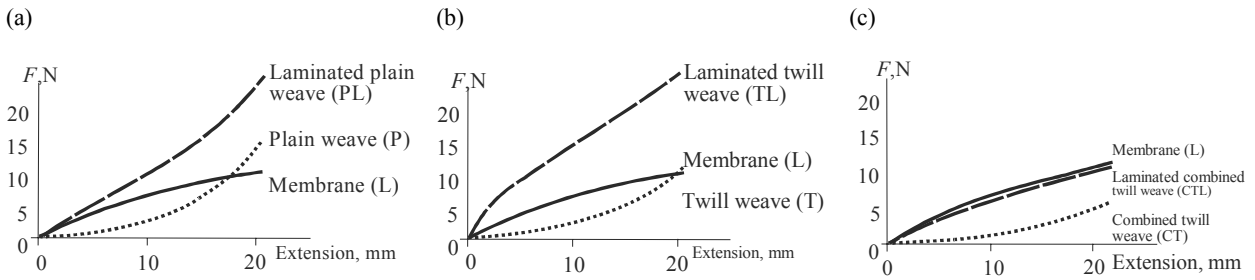


Fig. 5. The tension curves of fabrics, polymer membrane (L), and laminated materials: (a) plain weave samples (P), (b) twill weave samples (T), (c) combined twill weave (CT) samples.

Table 2. The views of local deformation zones in the bias specimen estimated on the basis of parameter Δb_{ij} variation

Code	Elongation of woven material				Code	Elongation of laminated woven material			
	$\epsilon_i = 5\%$	$\epsilon_i = 10\%$	$\epsilon_i = 15\%$	$\epsilon_i = 20\%$		$\epsilon_i = 5\%$	$\epsilon_i = 10\%$	$\epsilon_i = 15\%$	$\epsilon_i = 20\%$
P					PL				
T					TL				
CT					CTL				

Scale of measurements, %

--	--	--	--	--	--	--	--	--	--

deformation zones of the T specimen are wider and shorter. The height of the deformation zones of the CT specimen is similar to the one of P, although the width of deformation zones extends through the whole width

of the specimen. As the deformation increases up to $\epsilon_i = 20\%$ new deformation zones show up, concentrating around the central part. Comparison of the pictures of non-laminated and laminated samples (Table 2)

reveals that the lamination of the tested fabrics has changed the nature of the formation of deformation zones; the zones of uniform deformations are more spread and do not concentrate within the centre of the specimen.

Analysis of the maximum values Δb_{ij} and Δh_{ij} of laminated and non-laminated specimens (Tables 3, 4) shows that the influence of lamination is more evident within the T and CT specimens. The length of thread floats is higher for twill weave fabric, therefore samples T and CT are more flexible and the structure of those materials is less stable. As during lamination the movements of warp and weft threads are limited, deformation of points in transverse direction decreased 2.5 times on average within specimen CT and 4 times within specimen T, in longitudinal direction 1.56 times within specimen T and 1.26 times within specimen CT. Our investigation revealed that the change in the grid points width Δb decreased up to 1.96 times and the change in the height Δh decreased up to 1.1 times within specimen P.

It was estimated that during tension laminated bias specimens did not buckle when the total specimen elongation reached a maximum limit of $\varepsilon_i = 20\%$. At the same time non-laminated specimen P buckled at the elongation $\varepsilon_i = 10\%$, specimen T at $\varepsilon_i = 12\%$, and specimen CT at $\varepsilon_i = 14\%$.

In order to compare the behaviour of the investigated samples during tension, diagrams of Δb_{ij} , Δh_{ij} variation were drawn for non-laminated and laminated

samples (diagrams of the twill weave sample presented in Figs 6, 7). While the elongation ε of non-laminated fabric increases, Δh_{ij} within the width of the specimen changes only little, whereas marginally higher values of Δh_{ij} are noted in the centre of the specimen (Fig. 6a). Variation in Δb_{ij} is more evident and the peak of Δb_{ij} is fixed in the centre of the specimen (Figs 6a, 7a). The same tendency persists during the entire tension process. While the variation in the same characteristics within laminated samples is observed, the essential influence of lamination towards the performance of materials is estimated (Figs 6b, 7b). Variation in both Δb_{ij} and Δh_{ij} values was insignificant. No peaks were evident within the centre of the specimen, i.e. the stability of the sample increased and no buckling occurred during stretching of the laminated bias sample.

In order to evaluate the ratio of deformations more precisely, Poisson's ratio was calculated for each point of the stretched specimen $\mu_{ij} = \Delta b_{ij} / \Delta h_{ij}$ (Figs 8, 9). During tension Poisson's ratio in transverse to tension specimen middle line varies from 0.78 to 0.90 and in the tension direction – from 0.78 to 1.04. The estimated change in Poisson's ratio proves uneven performance of the bias woven specimen during uniaxial tension and its values depend on the position of the point and specimen elongation. In laminated samples the limits of Poisson's ratio (Figs 8b, 9b) varies from 0.87 to 1.00 and shows a more uneven deformation nature after the movement of fabric threads is restricted by lamination.

Table 3. Maximum values of the Δb_{ij} parameter

Code	$\Delta b_{i5}, \%$		$\Delta b_{i10}, \%$		$\Delta b_{i15}, \%$		$\Delta b_{i20}, \%$	
	Non-laminated	Laminated	Non-laminated	Laminated	Non-laminated	Laminated	Non-laminated	Laminated
P	-8.28	-5.75	-21.54	-14.42	-36.17	-19.41	-48.50	-24.74
T	-10.21	-2.45	-25.45	-4.88	-40.56	-7.32	-48.62	-11.11
CT	-9.87	-4.20	-23.67	-1.74	-35.59	-13.97	-43.06	-14.94

i – index values of the central part B of the specimen.

Table 4. Maximum values of the Δh_{ij} parameter

Code	$\Delta h_{i5}, \%$		$\Delta h_{i10}, \%$		$\Delta h_{i15}, \%$		$\Delta h_{i20}, \%$	
	Non-laminated	Laminated	Non-laminated	Laminated	Non-laminated	Laminated	Non-laminated	Laminated
P	3.82	8.27	11.54	12.36	20.38	21.49	25.97	23.67
T	7.85	5.01	13.26	7.59	18.88	12.64	22.95	16.00
CT	9.14	6.59	13.90	11.85	20.92	16.56	24.80	20.45

i – index values of the central part B of the specimen.

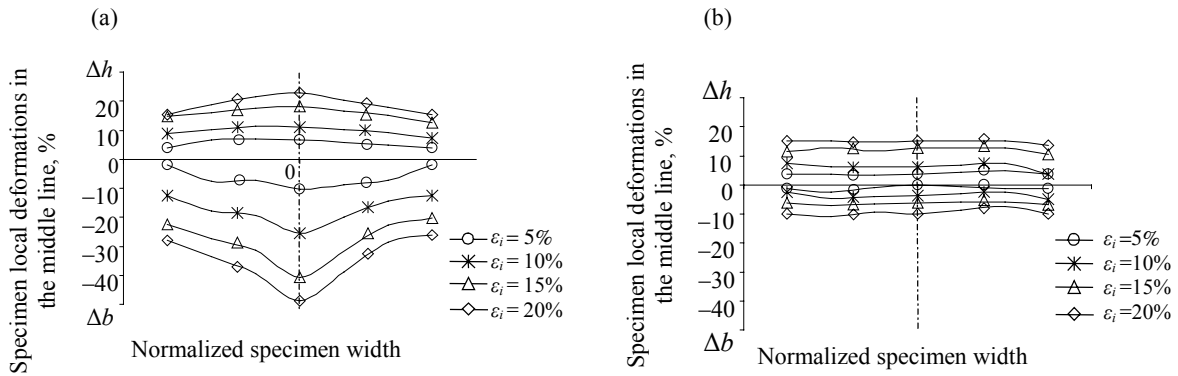


Fig. 6. Maximum deformations in the middle line of the bias specimen: (a) twill weave, (b) laminated twill weave.

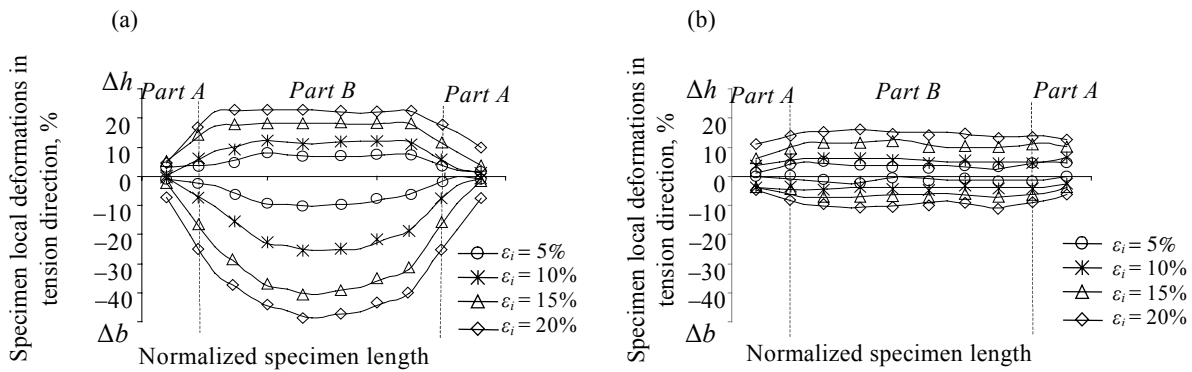


Fig. 7. Maximum deformations in the tension direction of the bias specimen: (a) twill weave, (b) laminated twill weave.

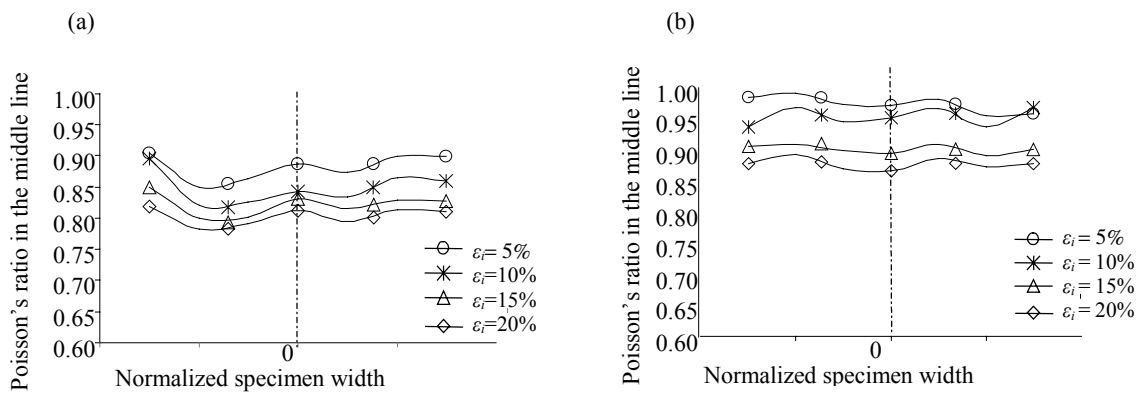


Fig. 8. Changes in Poisson's ratio in the middle line of the specimen: (a) twill weave, (b) laminated twill weave.

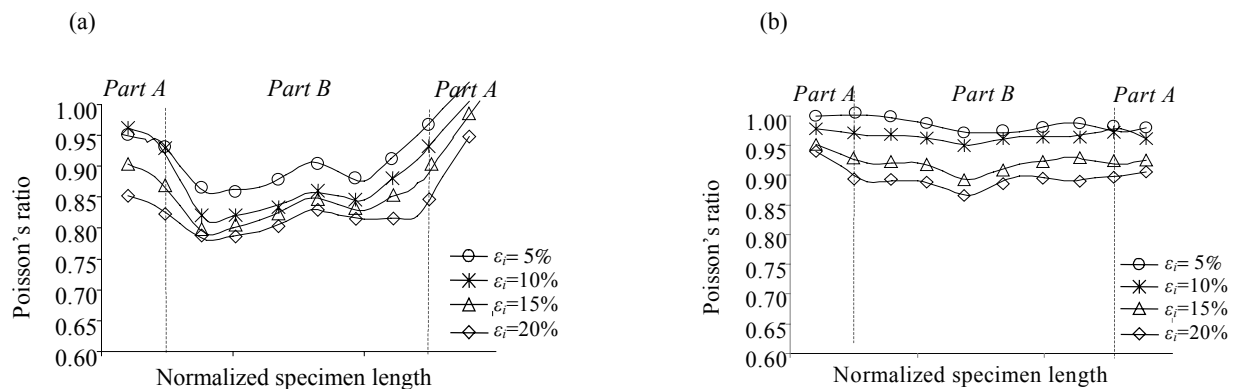


Fig. 9. Changes in Poisson's ratio in the tension direction of the specimen: (a) twill weave; (b) laminated twill weave.

5. CONCLUSIONS

Using the proposed image analysis method, local deformations of the tensioned bias woven specimen in transverse and longitudinal directions were estimated and regularities of variation in uniform deformation zones were assessed. Clear zones of uniform deformation appear and the number of these zones increases when the specimen elongates.

The proposed digital image-based methodology can be applied to study the behaviour of various materials. Comparison of the behaviour of materials shows that increase in bending rigidity changes the deformation character of laminated materials. For non-laminated low flexure rigidity materials the formation of localized deformation zones was estimated at primary stages of tension as in stiffer laminated fabric zones of uniform deformations are more spread and do not concentrate within the centre of the specimen. The analysis of local deformation values and zones explains the buckling phenomenon of bias stretched woven material and shows an increase in woven material stability after lamination.

The obtained results indicate that the used image analysis method and parameters well reflect the behaviour of the investigated materials and could also validate traditional models of mechanical analysis of textile materials more conveniently.

REFERENCES

- Barrientos, B., Martinez, R. A., Celorio, L. M., Lopez, J., and Cywiak, M. D. Measurement of out-of-plane deformation by combination of speckle photography and speckle shearing interferometry. *Int. J. Light Electron Opt.*, 2004, **115**, 248–252.
- Arial, Y., Shimamura, R., and Yokozeki, S. Dynamic out-of-plane deformation measurement using virtual speckle patterns. *Opt. Laser Eng.*, 2009, **47**, 563–569.
- Hale, R. D. An experimental investigation into strain distribution in 2D and 3D textile composites. *Compos. Sci. Technol.*, 2003, **63**(15), 2171–2185.
- Domskiene, J., Strazdiene, E., and Bekampiene, P. Development and optimisation of image analysis technique for fabric buckling evaluation. *Int. J. Cloth. Sci. Tech.*, 2011, **23**(5), 329–340.
- Abrill, H. C., Millan, M. S., and Valencia, E. Influence of the wrinkle perception with distance in the objective evaluation of fabric smoothness. *Opt. A-Pure. Appl. Op.*, 2008, **10**(10), 1–10.
- Zhu, B., Yu, T. X., and Tao, X. M. Large deformation and slippage mechanism of plain woven composite in bias extension. *Compos. Part. A-Appl. S.*, 2007, **38**, 1821–1828.
- Vang, X., Georganas, D. N., and Petriu, E. M. Automatic woven fabric structure identification by using principal component analysis and fuzzy clustering. In *Proceedings of the I2MTC – IEEE Instrumentation and Measurement Technology Conference*, 2010, 590–595.
- Xin, B. and Hu, J. An image based method for characterising the mechanical behaviours of fabrics. Part I: the measurement of in-plane tensile behaviour. *Fibres. Text. East. Eur.*, 2008, **1**, 72–75.
- Pan, B., Qian, K., Xie, H., and Asundi, A. Two-dimensional digital image correlation for in-plane displacement and strain measurement: a review. *Meas. Sci. Technol.*, 2009, **20**, 1–17.
- Lee, W., Padvoiskis, J., and Cao, E. Bias-extension of woven composite fabrics. *Int. J. Mater. Forming.*, 2008, **1**, 895–898.
- Tores Arellano, M., Crouzeix, L., Douchin, B., and Collombet, F. Strain field measurement of filament-wound composites at $\pm 55^\circ$ using digital image correlation: an approach for unit cells employing flat specimens. *Compos. Struct.*, 2010, **92**, 2457–2464.
- Behera, B. K. *Image-Processing in Textiles*. The Textile Institute, Textile Progress, 2004.
- Bekampienė, P. and Domskienė, J. Analysis of fabric specimen aspect ratio and deformation mechanism during bias tension. *Mater. Sci.*, 2009, **15**, 167–172.

14. Jauffrès, D., Morris, C. D., Sherwood, J. A., and Chen, J. Simulation of the thermo stamping of woven composites determination of the tensile and in-plane shearing behaviours. *Int. J. Mater. Forming*, 2009, 1(2), 161–164.
15. Ahmet, H., Aydilek, G. M., and Tuncer, B. E. Use of image analysis in determination of strain distribution during geosynthetic tensile testing. *J. Comput. Civil. Eng.*, 2004, 18(1), 65–74.

Kujutisel põhinev meetod madala paindejäikusega materjalide uurimiseks

Jovita Dargienė, Dalia Lukšaitė ja Jurgita Domskienė

On kirjeldatud kujutise analüüsil põhinevat meetodit, et uurida kootud materjalide käitumist tõmbekatsel ja deformatsioonide jaotumist materjalis. Lokaalsete deformatsioonide kindlaksmääramiseks kasutati spetsiaalset arvutiprogrammi, mis digitaalkujutise kaudu analüüsis kangale trükitud ringide kuju muutumist kogu tõmbekatse jooksul. Selle meetodi abil võrreldi kolme erinevat lamineeritud ja lamineerimata kangaproovi ning leiti, et lamineeritud kangastel on deformatsioonid nii pikkuses kui ka laiuses ühtlasemalt jaotunud. Samuti jõuti järeldusele, et kujutise analüüsil põhinev meetod kirjeldab adekvaatselt uuritud materjalide käitumist ja on tekstiilmaterjalide katsetamisel edukalt kasutatav.